

# Noise-induced vortex reversal of self-propelled particles

Hanshuang Chen<sup>1,2</sup> and Zhonghuai Hou<sup>1\*</sup>

<sup>1</sup>*Hefei National Laboratory for Physical Sciences at Microscales & Department of Chemical Physics, University of Science and Technology of China, Hefei, 230026, Peoples Republic of China*

<sup>2</sup>*School of Physics and Material Science, Anhui University, Hefei, 230039, Peoples Republic of China*

(Dated: November 24, 2018)

We report an interesting phenomenon of noise-induced vortex reversal in a two-dimensional system of self-propelled particles (SPP) with soft-core interactions. With the aid of forward flux sampling, we analyze the configurations along the reversal pathway and thus identify the mechanism of vortex reversal. We find that statistically the reversal exhibits a hierarchical process: those particles at the periphery first change their motion directions, and then more inner layers of particles reverse later on. Furthermore, we calculate the dependence of the average reversal rate on noise intensity  $D$  and the number  $N$  of SPP. We find that the rate decreases exponentially with the reciprocal of  $D$ . Interestingly, the rate varies nonmonotonically with  $N$  and a minimal rate exists for an intermediate value of  $N$ .

PACS numbers: 05.65.+b, 87.18.Tt, 64.60.-i

In recent years, the collective dynamics of self-propelled particles (SPP) has been a subject of intense research due to the potential implications in biology, physics, and engineering (see [1] for a recent review). Examples of SPP are abundant including traffic flow [2], birds flocks [3, 4], insects swarms [5, 6], bacteria colonies [7, 8], and active granular media [9, 10], just to list a few. Especially, inspired by the seminal work of Vicsek *et al.* [11], many theoretical and experimental studies reported that various systems of SPP can exhibit a wealth of emergent nonequilibrium patterns like swarming, clustering and vortex [12–18].

A fascinating phenomenon about SPP is that they can abruptly change their collective motion pattern, which may be induced by either intrinsic stochasticity such as error in communication among SPP or a response to an external influence such as a predator. For example, a recent experiment showed that marching locusts can suddenly switch their direction without any change in the external environment [5]. Later, the experimental results are further explained theoretically by a mathematical modeling, highlighting the nontrivial role of randomness or noise on this transition [19]. Also, noise-induced transitions between translational motion and rotational motion of SPP have been observed [20–23]. However, the research on this topic is still in its infancy and deserves more investigations. In particular, investigation of the mechanisms about these transitions is lacking at present. As we know, identifying the underlying mechanisms is key to understanding and controlling the collective motion of SPP.

In this paper, we report an interesting phenomenon of noise-induced vortex reversal between two different rotational directions in a two-dimensional model of SPP interacting via Morse potential [17]. Vortex pattern has

been commonly observed in nature, such as fish, ants [24, 25], *Bacillus subtilis* [26], and *Dictyostelium* cells [27]. By virtue of a recently developed simulation method of rare event, forward flux sampling (FFS) [28], we analyze the intermediate configurations along the reversal path and compute average reversal rate. We find that an important statistical property of the vortex reversal, that is, the reversal first starts from peripheral particles and then gradually to inner particles, so that almost all particles change their rotational directions. Furthermore, we show that the reversal rate decreases exponentially with the inverse of noise intensity. Interestingly, the rate varies nonmonotonically with the number of particles and a minimal rate exists.

We consider  $N$  identical SPP in two-dimensional space with positions  $\vec{x}_i$ , velocities  $\vec{v}_i$  ( $i = 1, \dots, N$ ) and unit mass. The equations of motion read [17]

$$\begin{aligned} \dot{\vec{x}}_i &= \vec{v}_i, \\ \dot{\vec{v}}_i &= \left( \alpha - \beta |\vec{v}_i|^2 \right) \vec{v}_i - \sum_{j \neq i} \nabla_i U(|\vec{x}_i - \vec{x}_j|) + \sqrt{2D} \vec{\xi}_i \end{aligned} \quad (1)$$

where the first and second terms on right hand side (rhs) of Eq.2 represent self-propelled force and friction force, respectively, and the third term is pair interaction among SPP given by the generalized Morse potential

$$U(|\vec{x}_i - \vec{x}_j|) = C_r e^{-|\vec{x}_i - \vec{x}_j|/l_r} - C_a e^{-|\vec{x}_i - \vec{x}_j|/l_a}. \quad (3)$$

Here,  $l_a$  and  $l_r$  represent the attractive and repulsive potential ranges,  $C_a$  and  $C_r$  represent their respective amplitudes. The last term on rhs of Eq.2 is a stochastic force of intensity  $D$  that are independent of particle index and satisfy  $\langle \xi_{i,m}(t) \rangle = 0$  and  $\langle \xi_{i,m}(t) \xi_{j,n}(t') \rangle = \delta_{ij} \delta_{mn} \delta(t - t')$  with  $i, j \in 1, \dots, N$ ;  $m, n \in x, y$ .

The model exhibits diverse dynamic patterns, such as clumps, rings and vortex, for different model parameters. Here we set  $\alpha = 1.0$ ,  $\beta = 0.5$ ,  $l_a = 2.0$ ,  $l_r = 0.5$ ,  $C_a = 0.6$  and  $C_r = 1.0$ , which corresponds to the case of vortex. To distinguish two different rotational directions of vortex, we define average angular momentum of particles

\*Electronic address: hzhlj@ustc.edu.cn

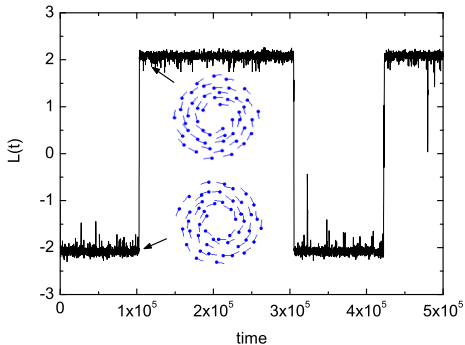


FIG. 1: (Color online) A long-time evolution of  $\bar{L}(t)$  at  $N = 40$  and  $D = 0.37$  shows several vortex reversals. The inset depicts two typical stable configurations of SPP: vortex with CW rotation ( $\bar{L} < 0$ ) and CCW rotation ( $\bar{L} > 0$ ).

$\bar{L}(t)$  as  $\bar{L}(t) = \frac{1}{N} \sum_{i=1}^N \bar{L}_i(t)$ , where  $\bar{L}_i(t) = \vec{x}_i(t) \times \vec{v}_i(t)$  is angular momentum of particle  $i$  at time  $t$ .  $\bar{L} < 0$  and  $\bar{L} > 0$  indicate that SPP rotate clockwise (CW) and counterclockwise (CCW), respectively. In the presence of a weak noise, vortex pattern is robust to noise.

Figure 1 shows a long-time evolution of  $\bar{L}(t)$  at  $N = 40$  and  $D = 0.37$ , obtained by numerically integrating Eqs.1,2 using a fourth order Adams-Bashforth method [29], allowing particles an infinite range of motion. One can observe that noise can induce the sudden transitions of SPP between two different rational directions. The inset in Fig.1 depicts two typical configurations of SPP: vortex with CW and CCW rotation. However, these transitions occur rarely and average waiting time between transitions is very long. In this situation, conventional brute-force simulation becomes highly inefficient. To overcome this difficulty, we will use FFS method of Allen and coworkers [28] to compute the rate of vortex reversal and evaluate statistical properties of the reversal path, which is the main purpose of the present work. FFS method was designed to study rare events both in and out of equilibrium. This method first defines an order parameter to distinguish between the initial state  $A$  and the final state  $B$ , and then uses a series of interfaces to force the system from  $A$  to  $B$  in a ratchet-like manner. Here, it is convenient to select  $\bar{L}$  as the order parameter, and consider CW vortex as  $A$  and CCW vortex as  $B$  without loss of generality because these two states are equivalent in our model.

By storing SPP configurations at each interface of FFS sampling, one can identify the statistical properties of the vortex reversal pathway. All results below are obtained by averaging 10 independent FFS samplings. In each FFS sampling, 1000 configurations in the center of mass coordinates are stored at each interface and are analyzed to obtain the statistical properties of the configurations. In Fig.2, we show the velocity field of SPP at six different

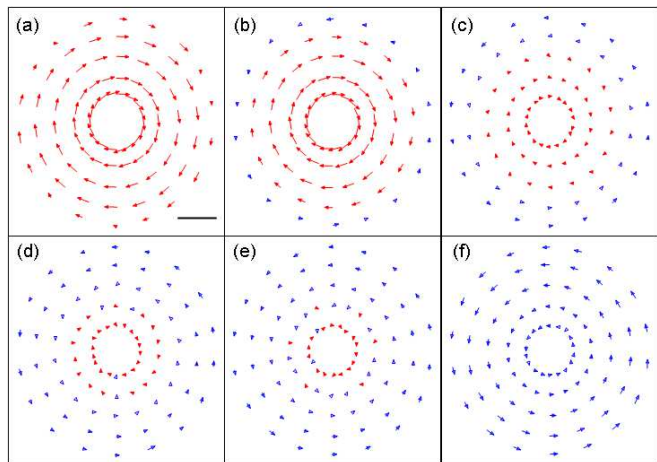


FIG. 2: (Color online) The velocity field of SPP at six different FFS interfaces, corresponding to (a)  $\bar{L} = -1.95$ , (b)  $\bar{L} = -1.6$ , (c)  $\bar{L} = 0$ , (d)  $\bar{L} = 0.25$ , (e)  $\bar{L} = 0.4$ , and (f)  $\bar{L} = 1.0$ , respectively. The bar in (a) indicates unit length.

interfaces. Fig.2(a) and Fig.2(f) show the velocity field before and after the reversal, indicating that the system is in stable vortex with CW and CCW rotation, respectively. While Figs.2(b-e) show the intermediate processes of the reversal. One can clearly observe that along the pathway of vortex reversal the velocity field gradually changes its sign from the periphery to center of the vortex. That is to say, vortex reversal first starts from peripheral particles and then gradually to inner particles, and finally almost all particles change original rational directions.

Further information on pathway of vortex reversal is provided by the radial distributions of average angular momentum  $\bar{L}(r)$  and average angular velocity  $\omega(r)$ , where  $r$  is the distance to the center of mass. In Fig.3, we plot  $\bar{L}(r)$  and  $\omega(r)$  for five different interfaces along the pathway of vortex reversal. From the variations of  $\bar{L}(r)$  and  $\omega(r)$  with interfaces one can observe that the whole process of the vortex reversal. Before the reversal ( $\bar{L} = -1.95$ ) the values of  $\bar{L}(r)$  and  $\omega(r)$  are always negative, irrespectively of  $r$ . That is, the system is in stable vortex with CW rotation before the reversal. When the reversal happens, for example, for  $\bar{L} = 0$  the values of  $\bar{L}(r)$  and  $\omega(r)$  become positive for  $r > 1.8$ , while for  $r < 1.8$  they are always negative. With increasing  $\bar{L}$  this situation further goes till any values of  $\bar{L}(r)$  and  $\omega(r)$  become positive. Finally, the vortex rotates with CCW direction. Therefore, this further validate that the statistical property of vortex reversal is that the reversal process starts from the periphery of the vortex. Also, we calculate the radial distributions of density of particles and the absolute value of velocity of particles, and find that they do not have significant difference with the interfaces  $\bar{L}$ .

It is informative to analyze the statistical properties

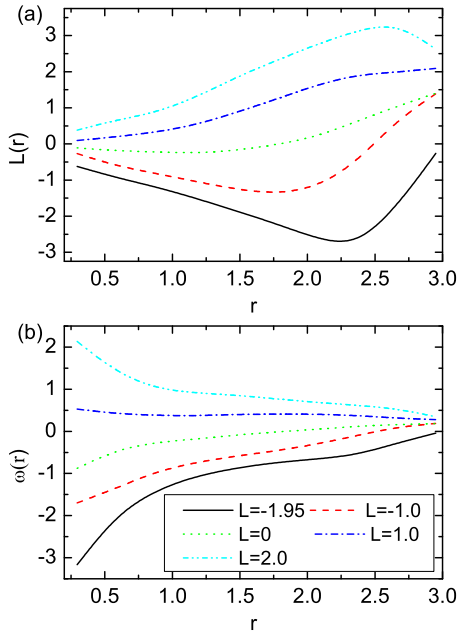


FIG. 3: (Color online) Radial distributions of average angular momentum  $\bar{L}(r)$  and average angular velocity  $\omega(r)$ , for five different interfaces along the pathway of vortex reversal.

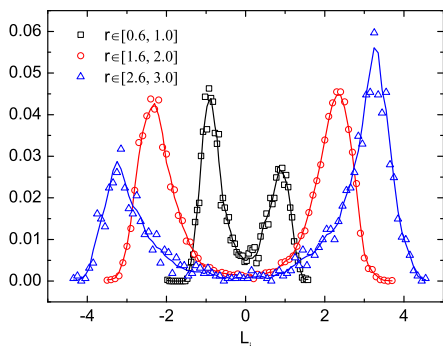


FIG. 4: (Color online) The distributions of angular momentum  $\bar{L}_i$  near the critical configurations for these particles with  $r \in [0.6, 1.0]$  (squares),  $r \in [1.6, 2.0]$  (circles), and  $r \in [2.6, 3.0]$  (triangles).

of critical configurations of SPP. Similar to definition in previous studies [30], the critical nucleus is determined by the committor probability  $P_B(i) = 0.5$ , where  $P_B(i)$  is the probability of reaching  $B$  state before returning to  $A$  state starting from the FFS interface  $i$ , which can be computed by FFS sampling. This shows that when the system initially locates at the critical configurations there is equal probability of returning to CW vortex or CCW vortex. We find that  $\bar{L} \simeq 0.08$  at the critical con-

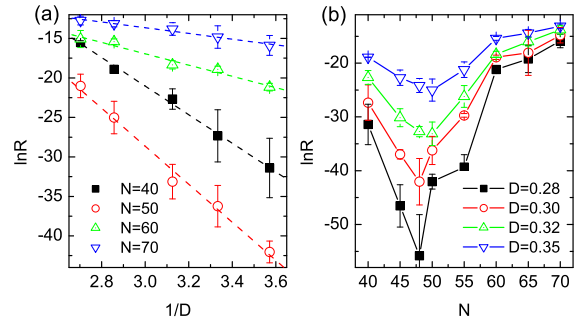


FIG. 5: (Color online) The natural logarithm of rate of vortex reversal  $\ln R$  as a function of the inverse of noise intensity  $1/D$  for different SPP number  $N$  (a) and as a function of  $N$  for different  $D$  (b). The dashed lines in (a) are plotted by linear fitting.

figurations, that is, the average angular momentum of all particles is slightly larger than zero at the critical configurations. By varying noise intensity  $D$  and the number of particles  $N$ , the value is not almost changed. Furthermore, we analyze the radial distributions of angular momentum  $\bar{L}_i$  of particles near the critical configurations. In Fig.4, we show that the distributions of  $\bar{L}_i$  of particles at  $r \in [0.6, 1.0]$  (squares),  $[1.6, 2.0]$  (circles), and  $[2.6, 3.0]$  (triangles). Interestingly, all these distributions are bimodal that are independent of  $r$ . The two peaks always correspond to  $\bar{L}_i < 0$  and  $\bar{L}_i > 0$ , respectively, separated by the lowest value of distributions located at about  $\bar{L}_i \simeq 0$ . But the loci of two peaks and their relative heights vary with  $r$ . For particles at the inner layer of vortex, the absolute values of  $\bar{L}_i$  is relatively low, meaning that the rotational property of these particles is weakened and thus become more disordered. While the other particles are of obvious rotation since the values of  $\bar{L}_i$  are comparable with ones at stable vortex. The first peak for  $\bar{L}_i < 0$  is higher at the inner layer of vortex, while the second peak for  $\bar{L}_i < 0$  is higher at the outer layer of vortex. At the center layer of vortex, the heights of the two peaks are nearly the same. The results give the properties of critical configurations and thereby further illustrate the mechanism of vortex reversal.

Another key question in vortex reversal concerns the dependence of average rate  $R$  of the reversal on noise intensity  $D$  and the number of particles  $N$ . The FFS method can give  $R$  as the production of the flux across the first interface and the conditional probabilities of reaching the last interface without returning the first interface. In Fig.5(a) we plot the natural logarithm of the rate  $\ln R$  as a function of the inverse of  $D$  for  $N$ . The results show that  $R$  decreases exponentially with  $1/D$ . It should be pointed out that in our simulation  $D$  is neither too large nor too small. We find that if  $D$  is larger than a critical value  $D_c \simeq 0.44$ , vortex pattern will be

destroyed, and thus vertex reversal makes no sense. If  $D$  is too small,  $R$  is very low so that simulation will be time-consuming. In Fig.5(b) we show that  $\ln R$  as a function of  $N$  for different  $D$ . Interestingly, we find that  $R$  varies nonmonotonically with  $N$ . There exists a minimal value of  $R$  at  $N = 48$  for low  $D$  and at  $N = 50$  for high  $D$ . From Fig.5(a), one may speculate that there seems to be an effective nonequilibrium potential for describing the collective transition in rotational directions. The potential barrier between CW vortex and CCW vortex is fixed if  $N$  is unchanged, such that the transition rate follow classical Kramers' law. On the other hand, the nonmonotonic dependence on  $R \sim N$  implies dependence of the effective nonequilibrium potential on  $N$  is nontrivial if exists. However, understanding these results from the view of theoretical analysis, if not infeasible, is at least a complex task at present.

In summary, using a two-dimensional model of SPP interacting via a soft-core potential, we have investigated the mechanism of noise-induced the changes of vortex pattern in rational direction. By virtue of FFS method we analyze the statistical property and compute the rate

of the reversal. We find that the reversal process is hierarchical: the process initially inspired by the peripheral particles, and those particles gradually drive more inner layers of particles into reverse motion directions. On the other hand, we show that the rate of the reversal decreases exponentially with the inverse of noise intensity. Interestingly, the reversal rate depends nonmonotonically on the number of SPP and a minimal rate exists at a moderate number of particles. Our findings may provide us some new understanding on the transitions of collective patterns of SPP.

### Acknowledgments

This work is supported by NSFC (Grant Nos. 91027012, 20933006). Z.H. acknowledges support by China National Funds for Distinguished Young Scientists (Grant No. 21125313). H.C. acknowledges support by the Doctoral Research Foundation of Anhui University (Grant No. KJ2012B042).

- 
- [1] T. Vicsek and A. Zafiris, e-print: arXiv:1010.5017 (2010).
  - [2] D. Helbing, Rev. Mod. Phys. **73**, 1067 (2001).
  - [3] A. C. *et al.*, Proc. Natl. Acad. Sci. U.S.A. **107**, 11865 (2010).
  - [4] K. Bhattacharya and T. Vicsek, New J. Phys. **12**, 093019 (2010).
  - [5] J. B. *et al.*, Science **312**, 1402 (2006).
  - [6] P. Romanczuk, I. D. Couzin, and L. Schimansky-Geier, Phys. Rev. Lett. **102**, 010602 (2009).
  - [7] L. Angelani, R. Di Leonardo, and G. Ruocco, Phys. Rev. Lett. **102**, 048104 (2009).
  - [8] E.-L. F. H. P. Zhang, Avraham Be'er and H. L. Swinney, Proc. Natl. Acad. Sci. U.S.A. **107**, 13626 (2010).
  - [9] S. R. V. Narayan and N. Menon, Science **317**, 105 (2007).
  - [10] J. Deseigne, O. Dauchot, and H. Chaté, Phys. Rev. Lett. **105**, 098001 (2010).
  - [11] T. Vicsek, A. Czirók, E. Ben-Jacob, I. Cohen, and O. Shochet, Phys. Rev. Lett. **75**, 1226 (1995).
  - [12] J. Toner and Y. Tu, Phys. Rev. Lett. **75**, 4326 (1995).
  - [13] G. Grégoire and H. Chaté, Phys. Rev. Lett. **92**, 025702 (2004).
  - [14] M. Aldana, V. Dossetti, C. Huepe, V. M. Kenkre, and H. Larralde, Phys. Rev. Lett. **98**, 095702 (2007).
  - [15] H. Chaté, F. Ginelli, and R. Montagne, Phys. Rev. Lett. **96**, 180602 (2006).
  - [16] H. Levine, W.-J. Rappel, and I. Cohen, Phys. Rev. E **63**, 017101 (2000).
  - [17] M. R. D'Orsogna, Y. L. Chuang, A. L. Bertozzi, and L. S. Chayes, Phys. Rev. Lett. **96**, 104302 (2006).
  - [18] F. Peruani, T. Klaus, A. Deutsch, and A. Voss-Boehme, Phys. Rev. Lett. **106**, 128101 (2011).
  - [19] C. A. Yates, R. Erban, C. Escudero, I. D. Couzin, J. Buhl, I. G. Kevrekidis, P. K. Mainia, and S. D. J. T, Proc. Natl. Acad. Sci. U.S.A. **106**, 5464 (2009).
  - [20] A. S. Mikhailov and D. H. Zanette, Phys. Rev. E **60**, 4571 (1999).
  - [21] U. Erdmann, W. Ebeling, and A. S. Mikhailov, Phys. Rev. E **71**, 051904 (2005).
  - [22] J. M. Allison Kolpas and I. G. Kevrekidis, Proc. Natl. Acad. Sci. U.S.A. **104**, 5931 (2007).
  - [23] J. Strefler, U. Erdmann, and L. Schimansky-Geier, Phys. Rev. E **78**, 031927 (2008).
  - [24] S. V. V. Julia K. Parrish and D. Grunbaum, Biol. Bull. **202**, 296 (2002).
  - [25] D. J. T. Sumpter, Phil. Trans. R. Soc. B **361**, 5 (2006).
  - [26] A. Czirók, E. Ben-Jacob, I. Cohen, and T. Vicsek, Phys. Rev. E **54**, 1791 (1996).
  - [27] W.-J. Rappel, A. Nicol, A. Sarkissian, H. Levine, and W. F. Loomis, Phys. Rev. Lett. **83**, 1247 (1999).
  - [28] R. J. Allen, P. B. Warren, and P. R. ten Wolde, Phys. Rev. Lett. **94**, 018104 (2005).
  - [29] G. H. Golub and J. M. Ortega, *Scientific Computing and Differential Equations: An Introduction to Numerical Methods* (Academic Press, 1992).
  - [30] A. C. Pan and D. Chandler, J. Phys. Chem. B **108**, 19681 (2004).